

Artificial neural networks analysis of entropy generation in magnetic-micropolar nanofluid flow equipped with porous media and Darcy-Forchheimer law

Zahoor Iqbal ^{a,b,c,*}, Md Fayz- Al- Asad ^f, Huiying Xu ^{a,**}, Xinzhong Zhu ^{a,d,e,l,***}, Muhammad Sajjad Hossain ^g, Ridha Selmi ^h, M.M. Alqarni ⁱ, Sharifah E. Alhazmi ^j, Fahima Hajjej ^k, M.M.H. Imran ^f

^a School of Computer Science and Technology, Zhejiang Normal University, Jinhua, 321004, China

^b Zhejiang Institute of Photoelectronics & Zhejiang Institute for Advanced Light Source, Zhejiang Normal University, Jinhua, Zhejiang, 321004, China

^c Department of Mathematics, Quaid-i-Azam University, Islamabad, 44000, Pakistan

^d Research Institute of Hangzhou Artificial Intelligence, Zhejiang Normal University, Hangzhou, 311231, China

^e College of Computer Science and Artificial Intelligence, Wenzhou University, Wenzhou, 325035, China

^f Department of Mathematics, American International University - Bangladesh, Kuratoli, Khilkhet, Dhaka, 1229, Bangladesh

^g Department of Arts and Sciences, Ahsanullah University of Science and Technology, Dhaka, 1208, Bangladesh

^h Department of Mathematics, College of Science, Northern Border University, Arar, Saudi Arabia

ⁱ Department of Mathematics, College of Sciences, King Khalid University, Abha, 61413, Saudi Arabia

^j Mathematics Department, Al-Qunfudah University College, Umm Al-Qura University, Mecca, Kingdom of Saudi Arabia

^k Department of Information Systems, College of Computer and Information Sciences, Princess Nourah Bint Abdulrahman University, P.O.Box 84428, Riyadh, 11671, Saudi Arabia

¹ Zhejiang Key Laboratory of Intelligent Education Technology and Application, Zhejiang Normal University, Jinhua, 321004, Zhejiang, China

ARTICLE INFO

Handling Editor: Dr Y Su

Keywords:

Non-linear thermal diffusion
Micropolar nanofluid
Porous media
Artificial neural networks
Entropy minimization
Keller-box technique
Bejan number

ABSTRACT

Understanding heat transfer rate, friction factor and mass transfer rate is crucial for optimizing energy and mass system. Since the majority of these phenomena involve heating and cooling, minimizing entropy creation is crucial. We investigate the thermal diffusion features in micropolar nanofluid across a porous medium with steady and incompressible, laminar flow with variable properties of magnetic field, thermal and mass expansion coefficient and we thoroughly examine the generation of entropy while considering its extensive applicability in industrial and engineering processes. Within the flow, the effects of Brownian motion through the nonlinear sheet, thermal and concentration convection, micropolar rotation, and magnetohydrodynamics have all been taken into consideration. By using the appropriate magnitude analysis, the governing partial differential equations are transformed into a system of ordinary differential equations. The Keller-Box technique is utilized to discretized the differential equations and ANN-LMBP technique is applied for the prediction of non-dimensional physical quantitates. These non-dimension data set is divided into three part: 80 % for training, 10 % for testing and 10 % for validation. An optimal solution is achieved at epoch 31 with MSE 2.4187×10^{-5} . We have obtained R values for training, testing, validation and overall are 0.99926, 0.99992, 0.99999 and 0.99944. A brief review of the flow profile, entropy minimization, and Bejan number

* Corresponding author. School of Computer Science and Technology, Zhejiang Normal University, Jinhua, 321004, China.

** Corresponding author.

*** Corresponding author. School of Computer Science and Technology, Zhejiang Normal University, Jinhua, 321004, China.

E-mail addresses: izahoor@math.qau.edu.pk (Z. Iqbal), xhy@zjnu.edu.cn (H. Xu), zxz@zjnu.edu.cn (X. Zhu).

<https://doi.org/10.1016/j.csite.2025.105870>

Received 9 September 2024; Received in revised form 2 December 2024; Accepted 12 February 2025

Available online 25 February 2025

2214-157X/© 2025 The Authors. Published by Elsevier Ltd. This is an open access article under the CC BY license (<http://creativecommons.org/licenses/by/4.0/>).

for the various physical parameters, including the thermophoresis parameter, thermal and concentration buoyancy parameter, vertex thickness, Brownian parameter, magnetic parameter, Darcy number, and Eckert number have been discussed graphically. It is perceived that when the Darcy number (Da) rises, the velocity profile decreases but the thermal profile increases. Moreover, the coefficient of skin friction, Nusselt number and Sherwood number for different parameters are computed and depicted in the form of graphs also compared with the numerical solution and obtained absolute error for friction, Nusselt and Sherwood number are $1.6636e - 04$, $3.1979e - 03$, $1.2645e - 04$.

1. Introduction

The study of micropolar liquids has recently attracted the attention of researchers. This consideration arises from the fact that conventional Newtonian fluids fail to accurately represent the characteristics of fluid flow in diverse industrial applications and biological contexts. Viscosity effects in most surface flows, both internal and external, are limited to a thin flow zone called the boundary layer. Viscous effects typically become significant when fluids are moving over surfaces. Boundary layer theory is the most studied topic due to its different applications in diverse fields. The understanding of boundary layer behavior is very important in the study of pumps, turbines, aircraft, airfoil drag and lift, underwater submarines, heat exchangers, and many more. The boundary layer is an important topic in aerodynamics as it has a significant impact on the overall aerodynamic properties of a body, such as its lift and drag ([1–3]). A stretching sheet denotes a dynamic boundary that extends in one or multiple directions, commonly utilized in fluid dynamics to simulate flows in processes such as extrusion, wire drawing, and film production. The stretching sheet problem serves as a fundamental case for analyzing boundary layer behavior influenced by diverse physical effects [4,5]. Umair et al. [6] studied slip flow past a stretching bending sheet. Kartik et al. [7] examined heat and mass transfer of nanofluid across inclined cylinder. Madhu et al. [8] studied quadratic thermal radiation and activation energy across the sheet. The study of fluids with an internal microstructure is regarded as an intriguing and complicated subject in theoretical hydrodynamics. Micropolar fluids are a special type of non-Newtonian fluid with suspended particles. Eringen [9] is the first person who showed that micropolar fluids that exhibits internal structures. In this model, microscopic impacts that originating from the regional microstructure also micro-motion of liquid particles. The physical composition of these liquids is made up of solid particles that are arranged at random and suspended in highly viscous fluids that have a shear stress which is not axisymmetric. Micropolar fluids have numerous applications in the field of industrial: paints, lubricants, polymers, medial: human and animal blood colloidal suspensions, animal blood carrying deformable particles, environmental: sub-surface flow patterns, microorganisms' study, wind patterns, turbulence, cloud and weather patterns etc. and other sectors like suspension, liquid crystals [10–13]. Israr et al. [14], proposed the Reiner-Philippoff fluid (RPF) model in their study as a substitute for Newton's Law of viscosity. Porosity and Darcy-Forchheimer parameters increase the model's flow rate, and thermal slip has a beneficial impact on heat transfer. Schmidt number and chemical reaction parameters affect mass diffusion rate. Rehman et al. [15] applied Soret and Dufor effect on MHD Carreau fluid with Darcy-Forchheimer model. Also, the Darcy-Forchheimer model is consider in Refs. [16–19]. Chen et al. [20] considered unsteady flow over the boundary layer surface. In his later study [21] he considered hybrid nanofluid with slippage constraints. Rehman et al. [22] considered Williamson nanofluid model with bio-convective flow and non-linear radiation. Jamshed et al. [23] consider thermal radiative flux with Arrhenius effect for Carreau fluid.

Pasha et al. [24] studied the micropolar liquid flow between two plates using decomposition method and found positive co relation between heat transfer rates and fluid concentration with Peclet number. Physics at the micro-nanoscale cannot be solely explained by Navier-Stokes equations. Conversely, because MFD has more gyration degrees of freedom, it can naturally detect physical processes at microscopic and small scales. Chen et al. [25] proposed a suitable integrating Chorin's projection method and time-center split method for tracking unsteadiness forms Navier Stokes equation with the effect of micropolar factors and he used nearly 2nd accuracy on multiple space meshes. We cannot imagine our life without energy and entropy is a measurement of disorder or randomness in a thermodynamic system. Minimization entropy is essential for achieving thermodynamic equilibrium in heat transfer process. Conductivity as well as the thermal efficiency of the material can be increased through the use of nanoparticles to improve heat transport. By including nanoparticles in base fluids, we can increase the material's thermal conductivity while maintaining a minimum level of entropy formation. Alsaedi et al. [26] studied entropy minimization in magneto-hydrodynamics Eyring-Powell nanofluid flow over a linearly stretchable surface. Hayat et al. [27] investigated Darcy-Forchheimer nanofluid flow in the context of a curved stretched sheet and showed that higher curvature, porosity, and Brinkman numbers were associated with increased entropy generation. Higher estimates of the Brinkman number and slip parameter are associated with a decrease in the Bejan number. Lei et al. [28] performed a comparison of the total entropy generation rate, internal exergy loss, and exergy efficiency in the membrane reactor used for methanol synthesis through carbon dioxide hydrogenation. It has been found that minimizing the total rate of entropy creation is equivalent to minimizing the loss of internal exergy and maximizing the exergy efficiency while keeping the intake energy constant. Priyajit [29] studied entropy generation loss due to different physical parameters and showed that demonstrated that the center portion of the cavity's lower wall is a very suitable location for a heat and mass source to distribute throughout the whole cavity. Fatunmbi et al. [30] studied micropolar fluid in the presence of thermal radiation. The effects of entropy formation on fluid flow via an inclined channel with constant vortex viscosity, changing dynamic viscosity, and thermal conductivity were investigated by Singh et al. [31]. Different studies have been done on micropolar fluid [32–36].

In recent years, there has been a growing belief that utilizing models inspired by the knowledge of the structures and functions of

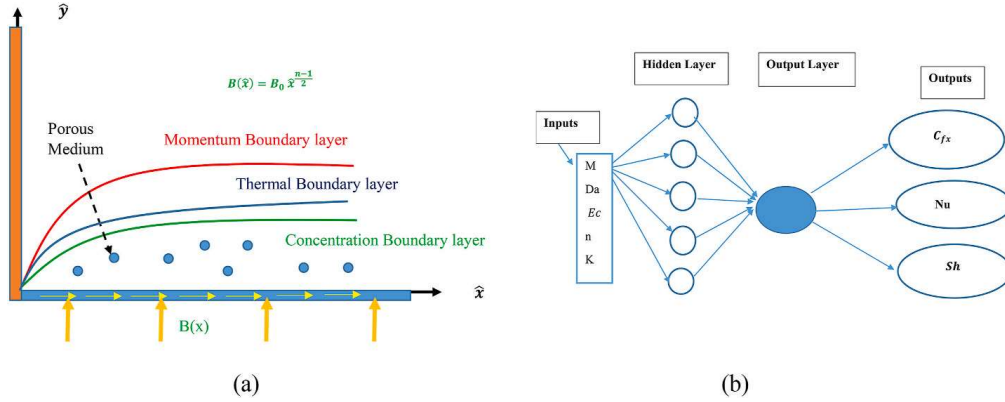


Fig. 1. (a) Physical model for micropolar fluid. (b) Artificial neural networks flow chart.

biological brain networks could be crucial in achieving success in dealing with complex tasks using artificial intelligence. The term used to refer to this emerging area of study is artificial neural networks (ANN). The machine has the potential to store prior knowledge and can intelligently anticipate future outcomes based on that knowledge [37,38]. Solving computational fluid dynamics models such as aerodynamic models, turbulence models, some specific flows, and mass and heat transfer using artificial intelligent (AI) is now the most crucial topics among the researchers [39]. Khan et al. [40] analyzed boundary layer theory using ANN technique, for that firstly, a data set was generated using numerical technique and then trained ANN model for different case to predict the thermal and velocity profile. Adrian et al. [41] predict the atmospheric boundary layer wind using ANN multilayer perceptron. He used three layers, first one is input layer which 6 nodes (input variables), for hidden layer he used 128 nodes and lastly output layer using 2 nodes that predicts the velocity in x, y direction. Raja et al. [42] studied Flaker- Scan systems using ANN method combine with GA (Genetic Algorithms)- AS (Active-Set) algorithms. Israr et al. [43] applied ANN model to predict heat transfer rate in bio convective flow. Sayed et al. [44] examined the numerical behavior of a ternary hybrid Carreau nanofluid in relation to thermal efficiency within an inclined magnetized environment.

From the above literature review, we were motivated to work with the micropolar nanofluid over the nonlinear stretching surface and work with the entropy generation for different physical parameters that are involved in our model equations. Our main focus is to minimize the entropy generation and deploy ANN methodology to predict the desired physical quantities such as Skin Friction coefficient, Nusselt number, Sherwood number. For this problem, ANN is chosen because they can approximate complex nonlinear relations also have advantages over numerical methods: ANNs can handle high-dimensional data and respond to changing problem dynamics without explicit mathematical formulation. ANNs solve problems quickly after training, making them useful for iterative simulations and real-time applications. While exact, finite difference and finite element approaches may need substantial processing resources and struggle with irregular geometries or discontinuities. Thus, ANNs were better for this investigation. Hopefully, this work will be beneficial in the study of micropolar fluid and other research. The novelty of this current work is here. Graphs depict and describe the effects of major variables in detail. Our main objective is to find the impact of MHD parameter, Eckert number, Darcy number on velocity, thermal profile and minimizing entropy generation.

The paper's nobility is outlined below.

- The magnetohydrodynamic and porous media play an important role in micropolar fluid flow; therefore, we introduced a magnetic term and porous effect in the momentum and energy equations.
- Considering entropy generation in the micropolar fluid flow will give us the ability to quantify the irreversibilities and inefficiencies of energy transformation, which will be beneficial for various applications in the industry as well as the medical sector.
- The ANN technique is proven to give better results than traditional statistical methods. ANN can predict the desired outcomes, whether the data set is large or small. For this study, training, testing and validation data were collected using numerical methods. We use this trained ANN model to predict the physical quantities of the problem.
- The ANN backpropagation algorithm uses Levenberg-Marquand for error minimization. It has second-order error accuracy, whereas the ADAM, gradient descent, and stochastic gradient descent methods have first-order error accuracy.

2. Mathematical model

We consider the two-dimensional micropolar nanofluid fluid flow, which is two dimensional, irrotational, steady, laminar flow over a darcy porous media. Here \hat{u} & \hat{v} is the fluid velocity in the x -direction and y -direction. We also consider that sheet is moving with velocity $u_w = a\hat{x}^n$ in the x -direction. We also consider porosity parameter, variable thermal and mass coefficient depend on x . Here, we adopt $k_{px} = k_p x^{n-1}$, $\beta_{tx} = \beta_t x^{2n-1}$ and $\beta_{cx} = \beta_c x^{2n-1}$ [45,46]. The flow geometry is depicted in Fig. 1(a).

With the above assumption, the model equations for this geometry can be written as [32,33,47].

Continuity Equation:

$$\frac{\partial \hat{u}}{\partial \hat{x}} + \frac{\partial \hat{v}}{\partial \hat{y}} = 0 \quad (1)$$

Momentum Equation

$$\hat{u} \frac{\partial \hat{u}}{\partial \hat{x}} + \hat{v} \frac{\partial \hat{u}}{\partial \hat{y}} = - \left(\frac{\mu + K}{\rho} \right) \frac{\partial^2 \hat{u}}{\partial \hat{y}^2} + \frac{\mu}{\rho} \frac{\partial \hat{N}}{\partial \hat{y}} - \left(\frac{\sigma B^2}{\rho} + \frac{v}{k_{px}} \right) \hat{u} + g \beta_{tx} (\hat{T} - T_\infty) + g \beta_{cx} (\hat{C} - C_\infty) \quad (2)$$

Micropolar Rotation:

$$\hat{u} \frac{\partial \hat{N}}{\partial \hat{x}} + \hat{v} \frac{\partial \hat{N}}{\partial \hat{y}} = - \left(\frac{K}{j\rho} \right) \left(2\hat{N} + \frac{\partial \hat{u}}{\partial \hat{y}} \right) + \frac{\gamma^*}{j\rho} \frac{\partial^2 \hat{N}}{\partial \hat{y}^2} \quad (3)$$

Energy Equation:

$$\hat{u} \frac{\partial \hat{T}}{\partial \hat{x}} + \hat{v} \frac{\partial \hat{T}}{\partial \hat{y}} = \left(\frac{k}{\rho c_p} \right) \frac{\partial^2 \hat{T}}{\partial \hat{y}^2} + \left(\frac{\mu + K}{\rho} \right) \left(\frac{\partial \hat{u}}{\partial \hat{y}} \right)^2 + \left(\frac{\sigma B^2}{\rho c_p} + \frac{v}{k_{px} c_p} \right) \hat{u}^2 + \Gamma \frac{\partial \hat{T}}{\partial \hat{y}} \left[\frac{D_T}{T_\infty} \frac{\partial \hat{T}}{\partial \hat{y}} + D_B \frac{\partial \hat{T}}{\partial \hat{y}} \frac{\partial \hat{C}}{\partial \hat{y}} \right] \quad (4)$$

Concentration Equation:

$$\hat{u} \frac{\partial \hat{C}}{\partial \hat{x}} + \hat{v} \frac{\partial \hat{C}}{\partial \hat{y}} = \frac{D_T}{T_\infty} \frac{\partial^2 \hat{T}}{\partial \hat{y}^2} + D_B \frac{\partial^2 \hat{C}}{\partial \hat{y}^2} \quad (5)$$

Here, \hat{u} & \hat{v} is the dimensional form of fluid velocity in \hat{x} & \hat{y} direction, \hat{N} is the micropolar rotation, \hat{T} is the temperature and \hat{C} is the mass concentration. $K, \mu, \rho, \sigma, \nu_p, \kappa_p, \beta_t, \beta_c, j, \gamma^*, k, c_p, D_B, D_T$ denote material parameter, viscosity, density, electrical conductivity, kinetic viscosity of porous media, porous medium permeability, thermal expansion coefficient, concentration expansion coefficient, micro inertia density, spin gradient viscosity, thermal conductivity, specific heat, thermal expansion, thermophoretic diffusion coefficient and Brownian diffusion coefficient respectively. $B(\hat{x}) = B_0 \hat{x}^{\frac{n-1}{2}}$ [46] is transverse magnetic field, s_0 is the surface boundary parameter, $(\cdot)_\infty$ denotes far stream property and $(\cdot)_w$ denotes near wall property.

With the boundary conditions [48,49]:

$$\left. \begin{array}{l} \hat{u} = ax^n, \hat{v} = 0, \hat{T} = T_w, \hat{N} = -s_0 \frac{\partial \hat{u}}{\partial \hat{y}}, \hat{C} = C_w \text{ at } \hat{y} = 0 \\ \hat{u} \rightarrow 0, \hat{v} \rightarrow 0, \hat{T} \rightarrow T_\infty, \hat{N} \rightarrow 0, \hat{C} \rightarrow C_\infty \text{ at } \hat{y} \rightarrow \infty \end{array} \right\} \quad (6)$$

Here, $a > 0$ constant and n nonlinear stretching parameter ($n = 1$ for linear stretching parameter), s_0 represents surface rotation parameter.

The physical quantities can be defined in the following form [49,46]:

$$\text{Skin friction coefficient, } C_f = \frac{2\tau_w}{\rho u_w^2}, \tau_w = \mu(1+K) \left(\frac{\partial \hat{u}}{\partial \hat{y}} \right)_{\hat{y}=0} + \mu K(\hat{N})_{\hat{y}=0} \quad (7)$$

$$\text{Nusselt Number, } Nu = \frac{x q_w}{k(T_w - T_\infty)}, q_w = -k \left(\frac{\partial \hat{T}}{\partial \hat{y}} \right)_{\hat{y}=0} \quad (8)$$

$$\text{Sherwood number, } Sh = \frac{x q_m}{D_B(C_w - C_\infty)}, q_m = -D_B \left(\frac{\partial \hat{C}}{\partial \hat{y}} \right)_{\hat{y}=0} \quad (9)$$

2.1. Entropy minimization

Entropy generation refers to the quantity of energy that is lost or wasted as a result of a process, which can lead to a decrease in the performance of engineering systems such as conduction and convection heat transfer rate. Entropy describes the randomness of molecular action in a microscopic system. Heat causes thermodynamic irreversibility and entropy grows according to the second rule of thermodynamics, which states that the entropy of a closed system never decreases. The system moves towards the highest entropy equilibrium configuration. Entropy formation denotes a reduction in energy quality and is significant in heat transfer studies. The existence of thermal radiation, porous medium fibers, viscous heating and changes in thermal conductivity as highlighted in the present hybrid magnetic nanofluid coating model, are all elements that lead to different sorts of irreversibility in the flow and thermal gradients.

For this physical model entropy generation (S_G [W/m^3K]) will in the following form [33,34]

$$S_G = \frac{1}{\hat{T}^2} \left(\frac{\partial \hat{T}}{\partial \hat{y}} \right)^2 + \frac{\mu + K}{\hat{T}} \left(\frac{\partial \hat{u}}{\partial \hat{y}} \right)^2 + \left(\frac{\sigma B^2}{\hat{T}} + \frac{\mu}{k_p \hat{T}} \right) \hat{u}^2 + \frac{D_B}{\hat{C}} \left(\frac{\partial \hat{C}}{\partial \hat{y}} \right)^2 + \frac{D_B}{\hat{T}} \frac{\partial \hat{T}}{\partial \hat{y}} \frac{\partial \hat{C}}{\partial \hat{y}} \quad (10)$$

2.2. Similarity solution

The following similarity transformations are used to reduce and non-dimensional the governing partial differential equations and boundary conditions: [46,50,51],

$$\eta = \sqrt{\frac{a(n+1)}{2\nu}} yx^{\frac{n-1}{2}}, \psi = \sqrt{\frac{2\nu ax^{n+1}}{n+1}} f(\eta), \theta = \frac{\hat{T} - T_\infty}{T_w - T_\infty}, \phi = \frac{\hat{C} - C_\infty}{C_w - C_\infty} \quad (11)$$

Here η is dimensionless transverse coordinate, ψ is stream function, $f(\eta)$ is a dimensionless stream function, $\theta(\eta)$ is dimensionless temperature and $\phi(\eta)$ is dimensionless concentration. Using definition of (11) we can find

$$u = \frac{\partial \psi}{\partial x} = ax^n f'(\eta), v = \frac{\nu \eta f(\eta)}{y} - \frac{n-1}{2} ax^{n-1} f'(\eta) \quad (12)$$

Using (11) and (12) Eq. (1)–(5) become

$$(1+K)f''' + ff'' - \frac{2n}{n+1}f'^2 + KN + \frac{2}{n+1}(Gr\theta + Gc\phi) - \frac{2}{n+1}(M+Da)f' = 0 \quad (13)$$

$$\left(1 + \frac{K}{2}\right)N'' + fN' - \frac{3n-1}{n+1}f'N - \frac{2K}{n+1}(2N + f'') = 0 \quad (14)$$

$$\theta'' + Pr \left(f\theta' + N_t\theta'^2 + NbNt\theta'\phi' + Ec(1+K)f'^2 + \frac{2}{n+1}(M+Da)f'^2Ec \right) = 0 \quad (15)$$

$$\phi'' + Le\phi'f + N_b\theta'' = 0 \quad (16)$$

And boundary conditions (6) become

$$\left. \begin{array}{l} f(0) = 0, f'(0) = 1, N(0) = s_0 f''(0), \theta(0) = 1, \phi(0) = 1 \\ f'(\eta) \rightarrow 0, N(\eta) \rightarrow 0, \theta(\eta) \rightarrow 0, \phi(\eta) \rightarrow 0 \text{ as } \eta \rightarrow \infty \end{array} \right\} \quad (17)$$

We found following nondimensional parameters: Thermal Grashof number, $Gr = \frac{g\beta_c(T_w - T_\infty)}{a^2}$, Concentration Grashof number, $Gc = \frac{g\beta_c(C_w - C_\infty)}{a^2}$, Magnetic number, $M = \frac{\sigma B_0^2}{a\rho}$, Darcy number, $Da = \frac{\nu}{ak_p}$, Eckert number, $Ec = \frac{u_w^2}{c_p(T_w - T_\infty)}$, Thermophoresis parameter, $Nt = \frac{\Gamma D_T}{T_\infty \nu}(T_w - T_\infty)$, Brownian parameter, $Nb = \frac{\Gamma D_C}{C_\infty \nu}(C_w - C_\infty)$, $Ntb = \frac{Nt}{Nb}$, Lewis number, $Le = \frac{\nu}{D_B}$.

Using the similarity variable, the desired physical quantities converted into the following non-dimensional form

$$\text{Skin friction, } C_{fx}(0) = (1 + (1 - s_0)K)f''(0) = \frac{c_f}{2} \sqrt{\frac{2Re_x}{n+1}} \quad (18)$$

$$\text{Nusselt Number, } -\theta'(0) = Nu \sqrt{\frac{2}{n+1}} Re_x^{-1/2} \quad (19)$$

$$\text{Sherwood Number, } -\phi'(0) = Sh \sqrt{\frac{2}{n+1}} Re_x^{-1/2} \quad (20)$$

From (10) using (8) we get dimensionless entropy generation

$$\begin{aligned} Ns &= \frac{n+1}{2(\Theta + \Omega)^2} Re\theta'^2 + \frac{(1+K)(n+1)}{2(\Theta + \Omega)^2} RePrEc f'' + \frac{(M+Da)RePrEc}{\Theta + \Omega} f'^2 + \frac{\Omega(n+1)}{2(\Theta + \Omega)} Re\phi'\phi' \\ &\quad + \frac{n+1}{2(\Phi + \varepsilon)} \gamma \varepsilon^2 Re\phi'^2 \end{aligned} \quad (21)$$

Here, Temperature relative parameter, $\Theta = \frac{(T_w - T_\infty)}{T_\infty}$, Concentration relative parameter, $\varepsilon = \frac{(C_w - C_\infty)}{C_\infty}$, Temperature ratio, $\Omega = \frac{T_w}{T_\infty}$.

Where first term represents Heat Transfer Entropy (HTE), the second term represents Fluid Friction Entropy (FFE), third term represents Magnetic and Darcy Force Entropy (MDE) and last two represent Diffusive Entropy (DIE).

2.3. Bejan Number

In thermal systems, Bejan number close to 1 indicates that *thermal* entropy generation is more dominant than *frictional* entropy generation in the overall entropy production. For $Be < 0.5$ the entropy generation produced by energy dissipation exceeds by that due to heat transfer. Bejan number can be defined following [52] as:

$$Be = \frac{\text{Entropy production due to thermal irreversibility}}{\text{Total entropy generation}}$$

$$Be = \frac{HTE + DIE}{NS}$$

$$Be = \frac{\frac{n+1}{2(\Theta+\Omega)^2} \text{Re}\theta'^2 + \frac{\Omega(n+1)}{2(\Theta+\Omega)} \text{Re}\theta'\phi' + \frac{n+1}{2(\Phi+\epsilon)} \gamma\epsilon^2 \text{Re}\phi'^2}{\frac{n+1}{2(\Theta+\Omega)^2} \text{Re}\theta'^2 + \frac{(1+K)(n+1)}{2(\Theta+\Omega)^2} \text{RePrEc}f'' + \frac{(M+Da)\text{RePrEc}}{\Theta+\Omega} f'^2 + \frac{\Omega(n+1)}{2(\Theta+\Omega)} \text{Re}\theta'\phi' + \frac{n+1}{2(\Phi+\epsilon)} \gamma\epsilon^2 \text{Re}\phi'^2} \quad (22)$$

3. Solution of the problem

3.1. Numerical computation

The system of non-linear differential equations is converted into group of first order ODEs as follows:

$$\begin{aligned} f' &= p \\ p' &= q \\ N' &= g \\ \theta' &= l \\ \phi' &= r \end{aligned}$$

$$q' = \left(\frac{1}{1+K} \right) \left[-fq + \frac{2n}{n+1} p^2 - Kg - \frac{2}{n+1} (Gr\theta + Gc\phi) + \frac{2}{n+1} (M+Da)p \right]$$

$$g' = \left(\frac{1}{1+\frac{K}{2}} \right) \left[-fg + \frac{3n-1}{n+1} pN + \frac{2K}{n+1} (2N+q) \right]$$

$$l' = -\text{Pr} \left(fl + N_t l^2 + N_b N_t lr + Ec(1+k)q^2 + \frac{2}{n+1} (M+Da)Ecp^2 \right)$$

$$r' = -(Lerf + N_b l')$$

The boundary conditions (17) reduce to:

$$f(0) = 0, p(0) = 1, \theta(0) = 1, \phi(0) = 1, g(0) = -s_0 q(0), p(\eta \rightarrow \infty) \rightarrow 0, \theta(\eta \rightarrow \infty) \rightarrow 0, \phi(\eta \rightarrow \infty) \rightarrow 0, N(\eta \rightarrow \infty) \rightarrow 0$$

The system of ODEs with the boundary conditions are solved with MATLAB by Keller-Box method.

The net rectangle is considered in the $\tau - \eta$ plane and the node points is defined by:

$$\tau^0 = 0, \tau^i = \tau^{i-1} + k_i, i = 1, 2, 3, \dots I$$

$$\eta^0 = 0, \eta_j = \eta_{j-1} + h_j, j = 1, 2, 3, \dots J$$

Where, k_i and h_j are respectively x and y spacing. For derivative we use following derivative

$$\frac{\partial u}{\partial \tau} = \frac{u^i - u^{i-1}}{k_i} \text{ in the } \tau \text{ direction and } \frac{\partial u}{\partial \eta} = \frac{u_j - u_{j-1}}{h_i} \text{ in the } \eta \text{ direction.}$$

$$\text{and for any points } (u)_j^{i-\frac{1}{2}} = \frac{1}{2} [(u)_j^i + (u)_{j-1}^{i-1}]$$

$$\text{for any points } (u)_{j-\frac{1}{2}}^i = \frac{1}{2} [(u)_j^i + (u)_{j-1}^i]$$

Then we apply Newtonian linearization method to linearize the non-dimensional system using following formula.

$$(u)_j^{k+1} = u_j^k + \delta u_j^k \text{ and neglect quadrating and higher term.}$$

The linearized differential equations of the ode system have a block tridiagonal form and solve using LU decomposition method. Starting solution for Keller Box method:

For this present problem we consider step size, $\Delta\eta = 0.02$ and initial guesses are taken in the following form [49]:

$$f = \eta - \left(\frac{\eta^2}{2\eta_\infty} \right), f' = 1 - \left(\frac{\eta}{\eta_\infty} \right), f'' = \frac{1}{\eta_\infty}$$

$$N = \frac{\eta}{\eta_\infty} - \left(\frac{\eta}{\eta_\infty} \right)^2, N' = \frac{1}{\eta_\infty} - \left(\frac{2\eta}{\eta_\infty^2} \right)$$

Table 1

Comparison of Nusselt number when ($M = 0, Ec = 0, Da = 0, n = 1, Pr = Le = 10, s_0 = 0, Gr = Gc = 0$)

Nt	Nb	- $\theta'(0)$		- $\phi'(0)$	
		Present	Khan [29]	Present	Khan [29]
0.1	0.1	0.952	0.952	2.12942	2.1294
0.2	0.2	0.3653	0.3654	2.5152	2.5152
0.3	0.3	0.1355	0.1355	2.6089	2.6088

Table 2

ANN-LMBP properties.

Properties	Hidden Layer	Neuron	Gradient	Momentum	Validation check	Maximum Epoch
Numbers	1	13	10^1	10^{10}	6	1000

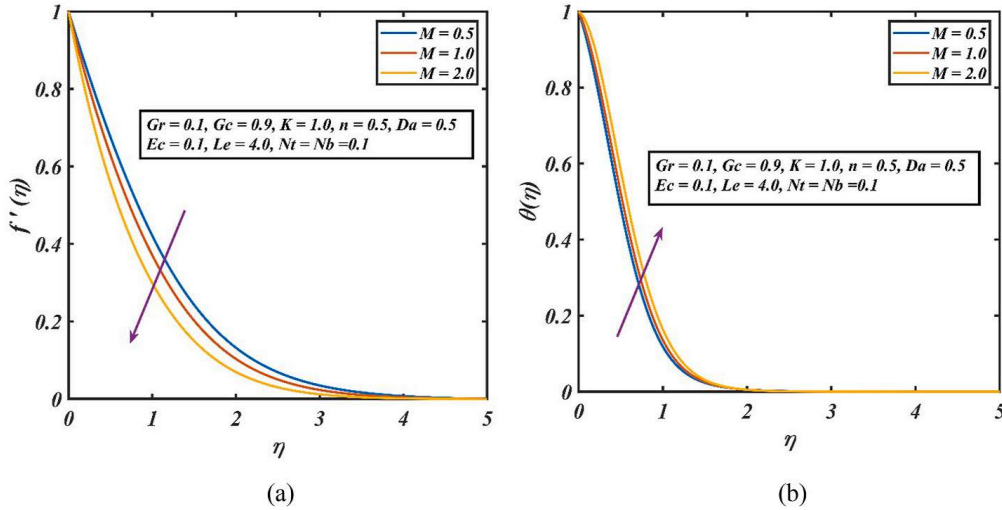


Fig. 2. Magnetic number impact on (a) velocity and (b) thermal profile.

$$\theta = 1 - \left(\frac{\eta}{\eta_\infty} \right), \theta' = \frac{1}{\eta_\infty}$$

$$\phi = 1 - \frac{\eta}{\eta_\infty}, \phi' = \frac{1}{\eta_\infty}$$

η_∞ is chosen between 5 and 10.

3.2. ANN computation

For Artificial Neural Network computing, a data set is generated for desired physical parameters: Skin Friction coefficients, Nusselt Number and Sherwood Number by varying input parameters: M, Da, Ec, n, K . Here we have used one hidden layer with 10 neurons. We split data sets 80% for training, 10% for testing and 10% for validation. We have used ‘Tansig’ as an activation and 2nd order error accuracy technique called Levenberg – Marquand method (see Table 1). The flow chart of ANN is depicted in Fig. 1(b).

Initial weights and biases chosen randomly and with LMBP these values updated in such way that optimality solutions arrived. In Table 2, Initially chosen properties of ANN and LMBP techniques are given.

4. Validation

For the present model we validate our results with the previous study of Khan and Pop [29].

From the above table we can ensure that results are in very close agreement. So that we can use this code for further implementation.

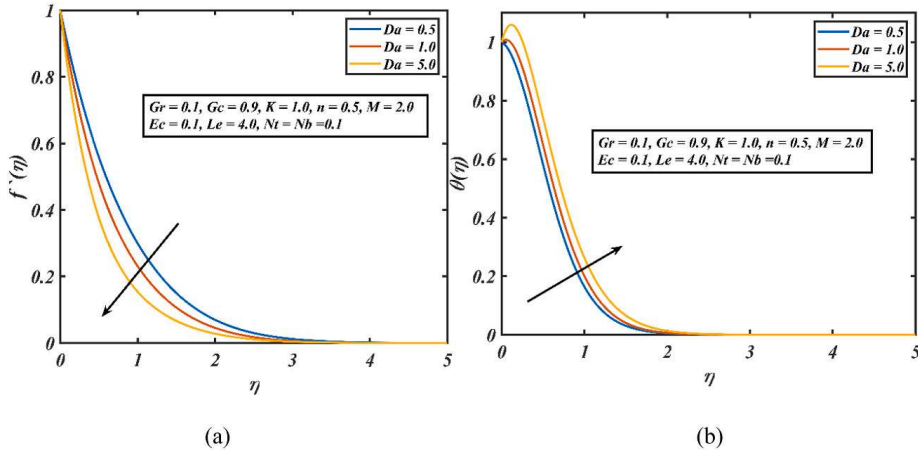


Fig. 3. Darcy number impact on velocity (a) and thermal (b) profile.

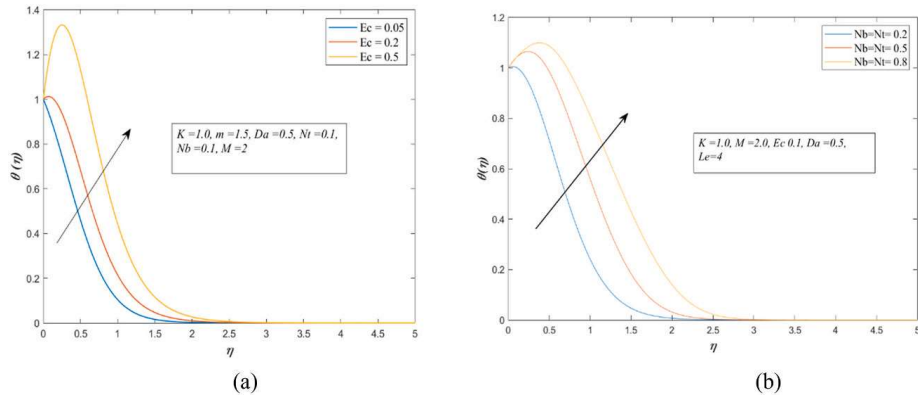


Fig. 4. Thermal Profile due to (a) Eckert Number and (b) Thermophoresis Brownian parameter.

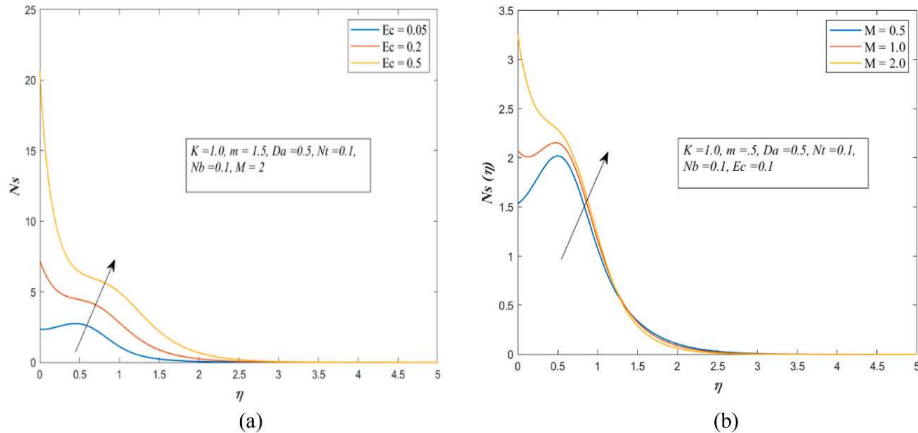


Fig. 5. Impact of Eckert number (a) and Magnetic parameter (b) on Ns .

5. Results and discussion

The impact of the parameters on flow profile, thermal profile, local entropy generation, Bejan number, heat transfer rates, Sherwood number and skin friction coefficient have been discussed graphically from Figs. 2–11. The parameter's value for this research have been choose from publish paper and physical applications. We have used fixed Prandtl number for this problem $Pr = 6.9$. And other changeable parameters are referred to the figure.

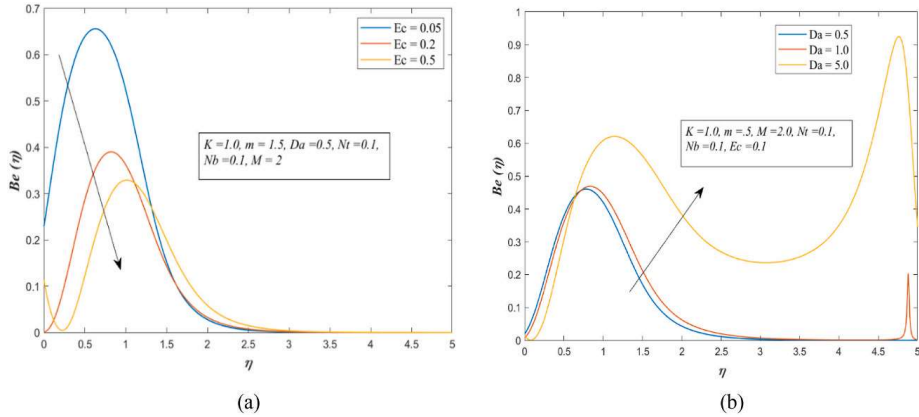


Fig. 6. Bejan number due to (a) Eckert number and (b) Darcy number.

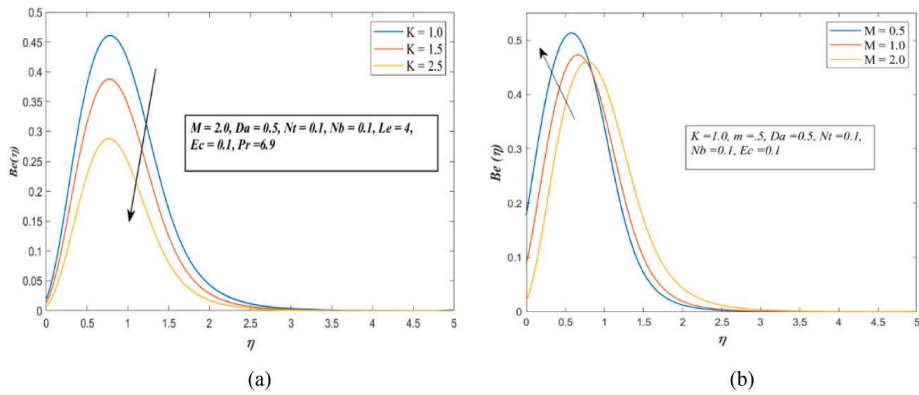


Fig. 7. Bejan Number due to (a) Material Parameter and (b) Magnetic number.

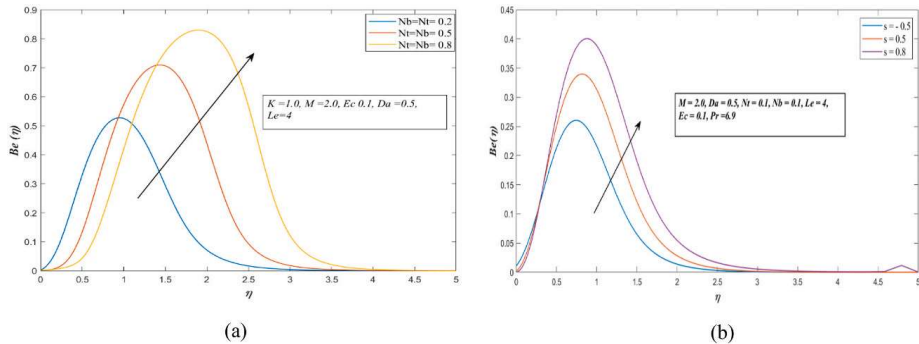


Fig. 8. Bejan Number due to (a) thermophysical parameters and (b) surface rotation.

5.1. Velocity and thermal profile

In this section we discuss the impact on different parameter on the velocity and thermal profile. The impact of M on the thermal and flow profiles is shown in figure (2). As we can see from this image, the Lorentz term in equation (10) resists the fluid flow motion perpendicular to it, while increasing the value of M the friction force becomes more dominant which results in the flow profile reducing as the magnetic number increases. The thermal profile exhibits opposite behavior when fluid velocity is suppressed, since a reduced velocity decreases convective heat transfer causing thermal boundary layer to thicken also this lowers the fluid's internal heat, making temperature gradients steeper and raising the thermal profile. Equation (15) demonstrates the positive impact for Joule heating term associated with the magnetic factor in the energy equation since the MHD induced Joule heating.

From figure (3), we observed that when the Darcy number (Da) rises, the velocity profile decreases but the thermal profile increases. This higher resistivity is caused by the inertial force in porous media becoming more important than the viscous force. In order to get over this, the resistivity velocity profile falls; however, in the case of the thermal profile, the temperature profile rises as a result of decreased fluid motion and convective heat transfer rate.

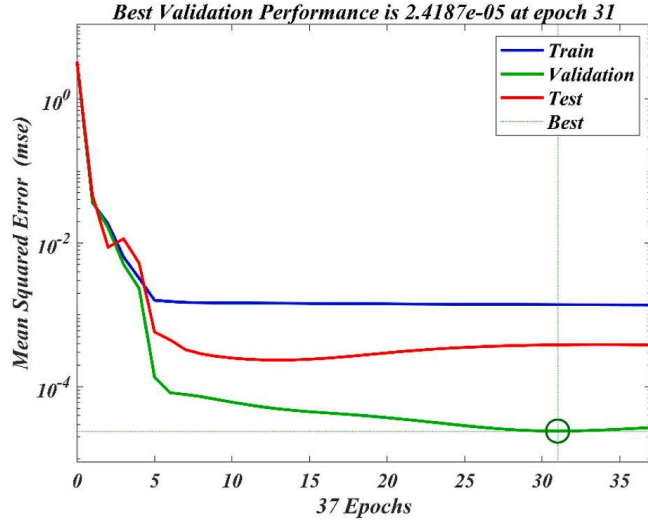


Fig. 9. Mean Square errors for the ANN computation.

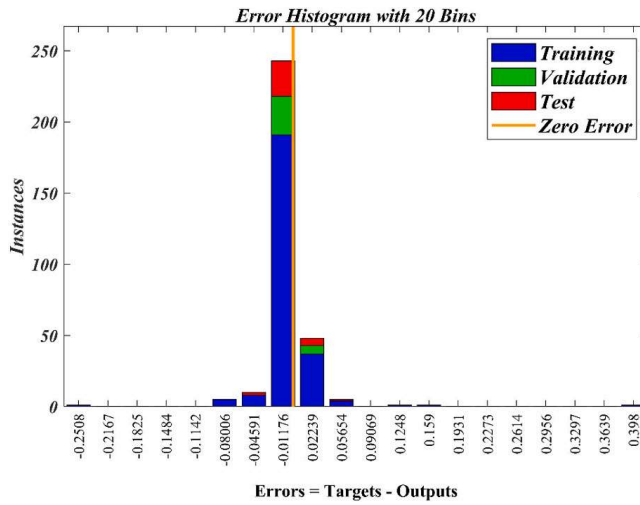


Fig. 10. Error Histogram for the ANN computation.

As we can see from Fig. 4(a), thermal profiles rise as the Eckert number rises. This is because a larger Eckert number means that kinetic energy becomes more important than enthalpy changes. The temperature profile in a fluidic system is dominated not only by temperature gradients in the system but also by dissipation from frictional forces in the fluid at high flow velocities. This will result in enhanced convective heat transfer and increase thermal profile. Again, in Fig. 4(b) thermophoresis and Brownian parameter shows positive impact on thermal profile. Nt represents the tendency of nanoparticles to mitigate from the wall surface to the surroundings. Increasing Nt mitigate more energy from wall as a result thermal profile increase. The impact of the random mobility of nanoparticles (caused by Brownian motion) on energy transfer is measured by the Brownian parameter. It is connected to both the fluid-nanoparticle interaction and thermal diffusion. Therefore, Brownian motion improves total energy transfer, thickens the thermal boundary layer, increases the random motion of nanoparticles, and increases the thermal conductivity of the nanofluid, which facilitates more uniform heat distribution and raises the thermal profile.

5.2. Entropy minimization and Bejan Number

In this section, we discuss entropy generation rate (Ns) and non-dimensional Bejan number for varying different physical parameters. From figure 5 (a, b) we plot Ns for Eckert number (Ec) and magnetic number (M). Initial Ns takes higher values for Eckert number than other parameters and Ec gives positive impact on Ns . This is because higher Eckert number always leads to increase fluid mixing and shear stress thus higher level of irreversibility as a result Ns rises. As well as Lorentz effect also gives positive impact on Ns . So, values of Ec number should be less to ensure the minimum entropy generation. Bejan number establishes a relationship between the fluid flow's mass transfer rate and heat transfer rate. It's the ratio of heat transfer coefficient to the mass transfer coefficient. In Figs. 6–8 we demonstrate the Bejan number for Eckert number, Darcy number, micropolar properties, magnetic number, thermo-physical parameter and micro rotational parameter. Initially at the near surface, Bejan number is low because of dominant viscous

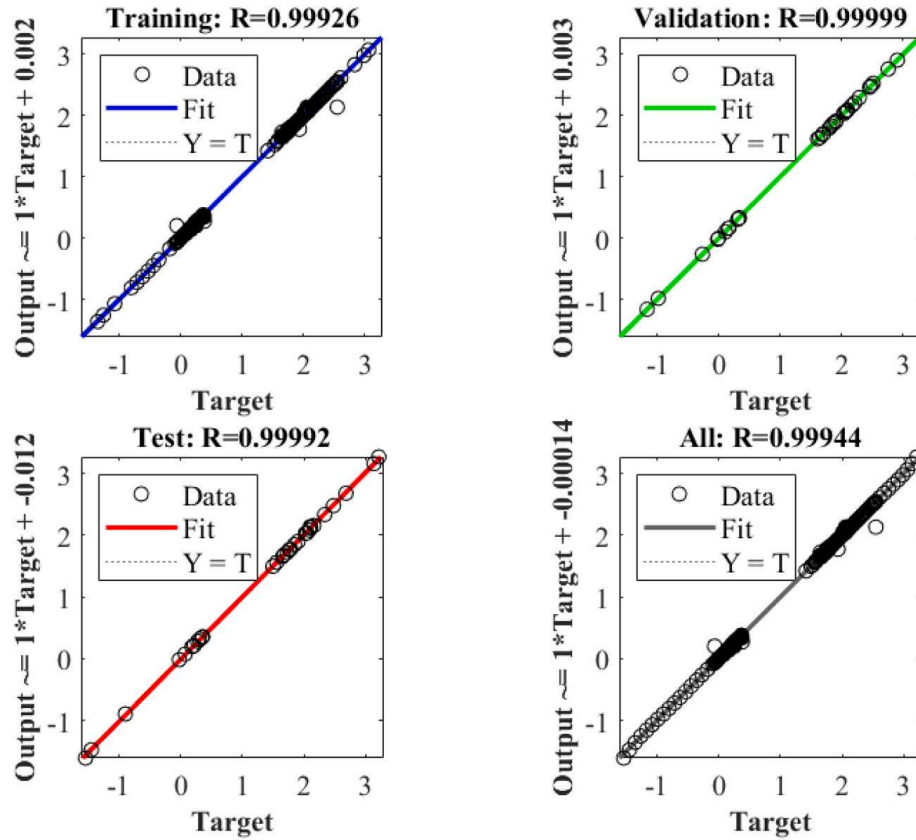


Fig. 11. Regression value for ANN computation.

effect with the boundary layer. Again, as we ascend from the surface wall, the effect of thermal transfer entropy along with diffusive entropy become more dominant than the others entropy generation effects. Increase boundary layer thickness affects the convective heat transfer rates and mass transfer rates. The effect of fluid friction entropy is low within this region. But far from the surface when boundary layer has fully developed the effect of convective heat transfer rate is becoming low thus decrease the Bejan number. From Fig. 6(a), we can conclude that by increasing Eckert number, Bejan number is decreasing. A more complex scenario can be seen in Fig. 6(b), due to the increasing effect of Darcy number. As Darcy number increase Bejan number is also increasing. Porous medium may play the crucial role for this complexity.

The impact of Bejan number for material parameter and the magnetic parameter is depicted in Fig. 7(a and b). We examined that the increasing trend of material parameter diminishes the Bejan number in Fig. 7(a). Additionally, we found that Bejan number give the positive impact due to Magnetic number. This is because the fact of the larger value of M results in a more noticeable frictional effect, which raises the fluid temperature and increases the Bejan number. Also, thermophysical properties and rotational factors increase the fluid temperature that causes the increasing factor of Bejan number. In Fig. 8(a and b), it is seen that the higher magnitudes of thermophysical parameter and surface rotation leads to builds up the Bejan number profiles.

5.3. ANN computation for desired physical properties

Artificial neural network (ANN) is an advanced computing model that learns from the previous data like our human brain and can predict the future results. ANN provides an alternative method over traditional methods like regression model, curve fitting. Where traditional methods failed to capture complex behavior and nonlinearity, ANN can handle complexity and nonlinearity using its supervised learning technique. To carry out the ANN methodology we have applied "tansig" activation function defined by $\text{tan}H = \frac{2}{1+e^{-2x}}$. This tansig function can handle non-linear relation between input and outputs also it provides smooth gradients ensure stable and effective learning during ANN training.

ANN has two processes.

- (i) Forwards Propagation
- (ii) Back ward propagation

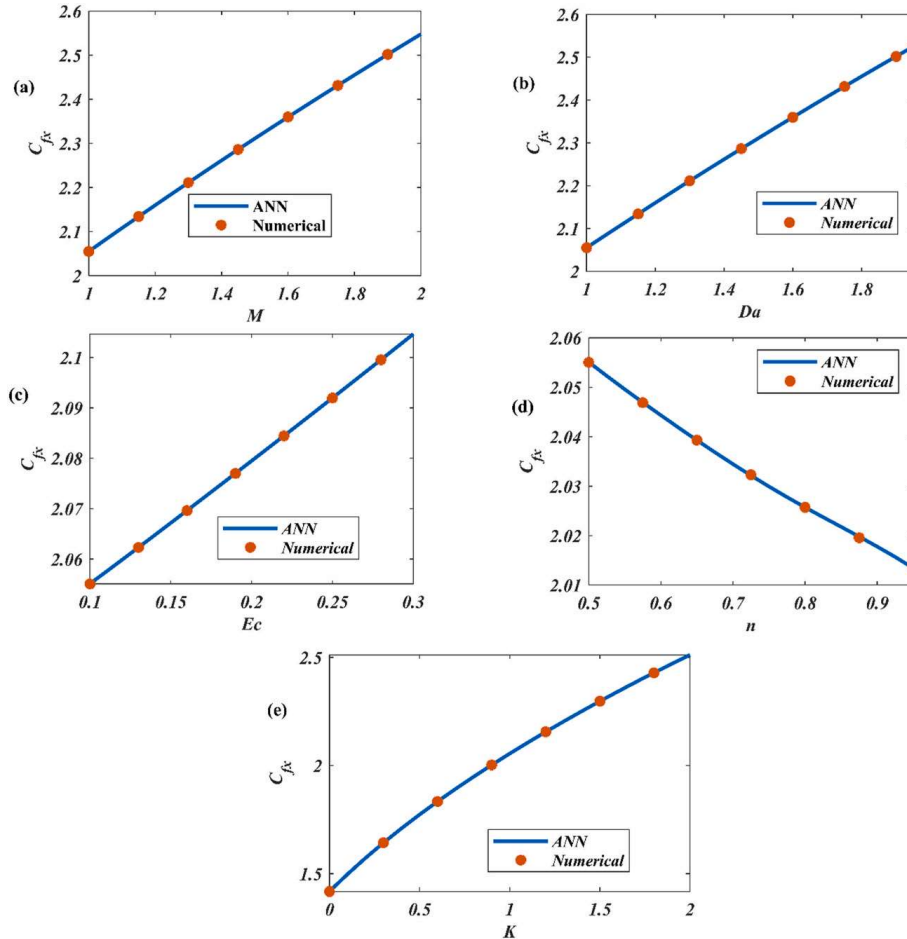
5.3.1. Forward propagation

The value input data is going through the model, and each neuron in the hidden layers calculates the weighted sum of its given

Table 3

ANN MSE properties in LMBP technique.

MSE Training	MSE Validation	MSE Testing	R^2 value (Training, Testing and validation)	Epoch	Time (sec)
$3.647e - 03$	$2.4187e - 05$	$3.8397e - 04$	0.99926, 0.99992, 0.99999	39	8

**Fig. 12.** Skin Friction value for different parameters.

input values and applies a non-linear or linear activation function to it. The output values are subsequently transmitted to the subsequent layer, and this cycle continues until we reach the output layer. Mathematically, information $y_i(x)$ enters the hidden layers for input layers. x, W, b, o represent inputs, weight, bias and outputs respectively. n is the number of neurons.

$$y_i(x) = \sum_{j=1}^n W1_{ij}x_j + b1_i$$

Hidden layer feeds the information of Input layer apply activation function over this $y_i(x)$ and the value of output layers is

$$y_o(x) = \sum_{j=1}^n W2_{ij}z_j + b2_i$$

5.3.2. Backward propagation

During this procedure, we evaluate the outcomes of artificial neural networks (ANN) by comparing them to the target values. The mean square error is calculated defined by

$$L = MSE = \frac{1}{n} \sum_{i=1}^n (y_i - \hat{y}_i)^2$$

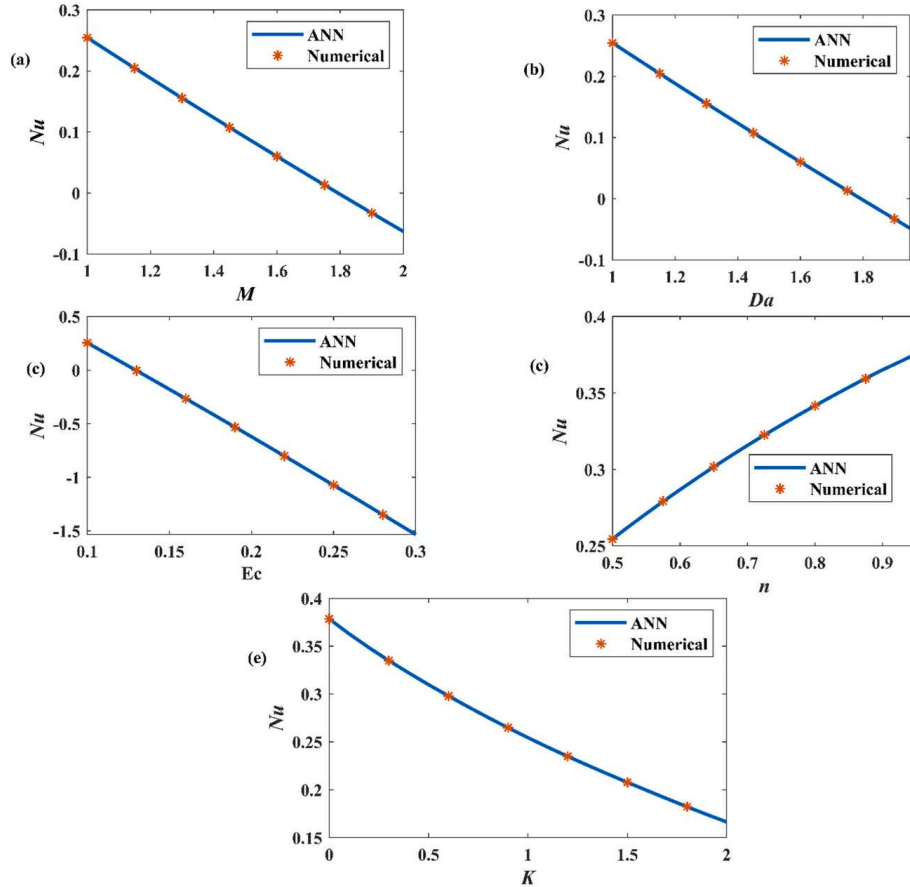


Fig. 13. Nusselt Number for different parameters.

The errors are computed and minimized through the 2nd order error minimization method (Levenberg-Marquardt). The Levenberg-Marquardt algorithm mainly consists of two popular numerical minimization algorithms: the gradient descent method and the Gauss-Newton method. It calculates the partial derivative of MSE loss with respect to weights and biases and update the initial W_i and b_i using following formula

$$W_i^{k+1} = W_i^k - \eta \frac{\partial L}{\partial W_i^k}$$

$$b_i^{k+1} = b_i^k - \eta \frac{\partial L}{\partial b_i^k}$$

Here, η is the learning rate.

Now, we have used this ANN methodology for predicting C_{fx} , Nu & Sh . In our ANN model we have 5 inputs, 10 neurons and 3 outputs.

In Table 3, we have ANN performance MSE values with number of epoch and time. The regression R^2 value is close to 1 in all cases. In Fig. 9, Mean square error is plotted against the epoch number, best validation performance is found 2.4187×10^{-5} at epoch 31.

In Fig. 10, we have plotted error histogram. The error is calculated from the predicted value of ANN and numerical solution. In Fig. 11, we have plotted output results against the target results and the regression value for training, testing and validation are calculate and shown top of the figure. We have used 80% of our data for training, in this case we have the regression value 0.99926, this is very close to 1 so data are perfectly fitting. For test data set we have the regression value 0.99992, this ensure that our ANN model is trained well and in the case of validation the value is 0.99999.

In Fig. 12, ANN predicted results are plotted with numerical results. Skin friction shows positive correlation with the parameter M , Da , Ec , k but opposite results for nonlinear stretching parameter (n). Skin friction coefficients increase for M because Lorentz force gives the opposite resistance force, this increases the coefficient force in the flow field. Da number extract extra inertial resistance as a results skin friction coefficient increases. In Fig. 13, we have the opposite observation that is heat transfer rate increase for non-linear stretching parameter and decrease for other cases. Nu is likewise observed to decrease with increasing Ec . Since greater viscous dissipation is induced with increasing Ec values, temperatures are boosted due to the conversion of mechanical energy into heat. This results in a net migration of heat from the wall to the hybrid nanofluid. In other words, heat transferred from the nanofluid to the wall (sheet) is reduced producing lower Nusselt numbers

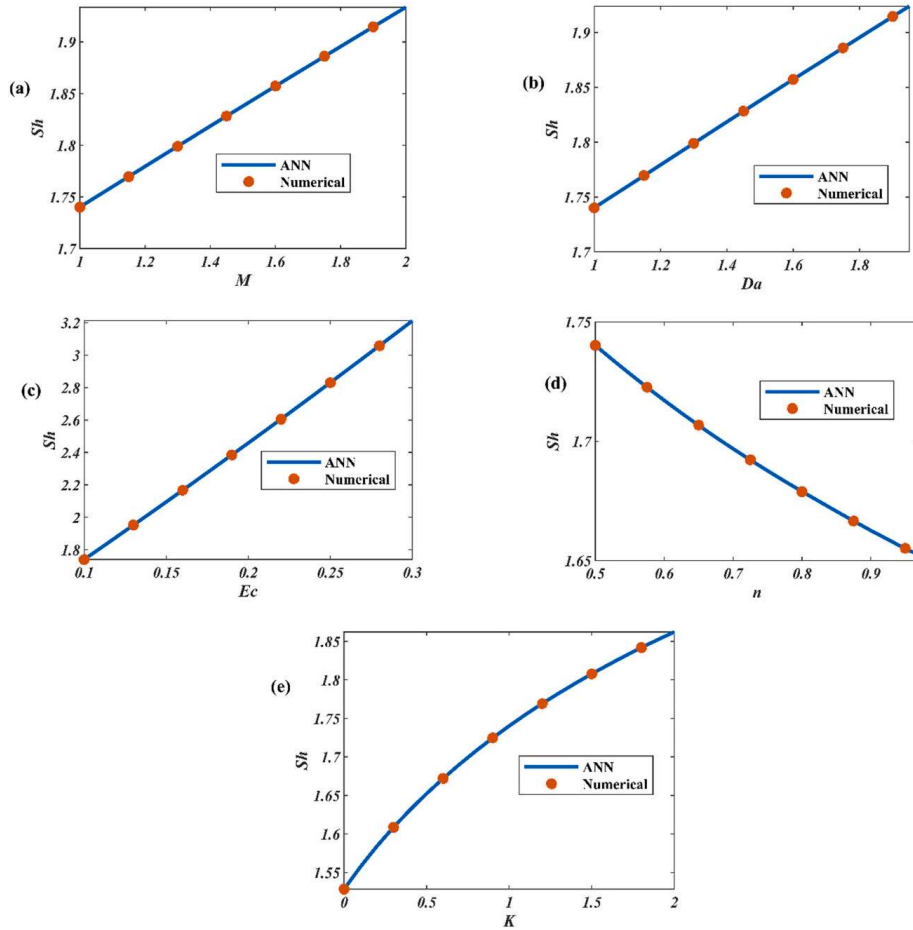


Fig. 14. Sherwood Number for different parameters.

Same reason can be drawn for Fig. 14, where M, Da, Ec, K gives the positive impact. When we increase the value of Da , flow becomes more complex sometimes leading to turbulent flow that enhance the mixing ratio of diffusion so the value of Sh increase. When the value of n is increased, the flow field gets more complicated, which results in an increase in flow curvature and intense mixing. Consequently, the value of Sh drops as a result of this greater mixing, which increases the convective mass transfer and reduces the importance of molecular diffusion.

6. Conclusion

In the present study, we consider micropolar nanofluid with the presence of MHD, buoyancy parameter, Brownian motion and diffusion parameter over the nonlinear stretching sheet. We also consider the entropy generation for this problem to ensure the minimum entropy generation. The governing boundary layer equations have been converted into system of nonlinear ordinary differential using some magnitude analysis. This nonlinear system of equations is tackled with numerical method and then ANN method is applied for the prediction of C_{fx} , Nu & Sh .

- Velocity profiles are decreasing for Magnetic parameter and Darcy number because extra resistance force due to applied Lorentz force and presence of porous media in the flow filed.
- Temperature profiles are increasing for magnetic numbers, Darcy number, Eckert number and thermophysical parameters. All these factors increase temperature gradient in the flow filed thus increasing thermal profile.
- Eckert number has maximum entropy generation over the flow filed, so we must have to ensure lower Eckert number for this problem. Also, Magnetic parameter increases the entropy generation.
- Bejan number is low near the wall and reaches its maximum value when we are moving up from the wall and last in the far filed Bejan number again decreasing but some complexity can be seen for Darcy number where Bejan number suddenly increase in the far filed then again decrease.
- Friction forces increasing with the increase of M, Da, Ec & K but decrease with n . Magnetic parameter and porosity Darcy number increase the frictional force as a result friction coefficient is increased. Nusselt increase with increasing n but decrease for other controlling parameters. Similar phenomena can be seen for Sherwood number.

(f) ANN predicted results shows good accuracy for the Skin friction coefficient, Nusselt number and Sherwood number. For these cases regression values are very close to 1.

ANN is proven to be an alternative statistical tool over tradition methods. But It also have some limitations, like to train the ANN model we need training data. Again, when more variation in data set then choosing optimal number of neurons or hidden layers is cumbersome. To overcome this situation one can, apply Physics Informed Neural Network where no prior data set is needed.

Also, one can easily, extended the study by consider the hybrid or tri-hybrid nanoparticles with different base fluid and adding more realistic boundary condition the work will be new path direction.

CRediT authorship contribution statement

Zahoor Iqbal: Writing – original draft, Software, Resources, Methodology, Investigation, Conceptualization. **Md Fayz- Al- Asad:** Writing – original draft, Resources, Methodology, Conceptualization. **Huiying Xu:** Funding acquisition, Validation, Writing – review & editing. **Xinzhong Zhu:** Validation, Software, Investigation, Data curation, Conceptualization. **Muhammad Sajjad Hossain:** Writing – original draft, Software, Methodology, Formal analysis, Conceptualization. **Ridha Selmi:** Visualization, Resources, Methodology, Formal analysis. **M.M. Alqarni:** Supervision, Funding acquisition, Formal analysis, Data curation. **Sharifah E. Alhazmi:** Visualization, Validation, Supervision, Software. **Fahima Hajjej:** Resources, Software, Validation, Writing – review & editing. **M.M.H. Imran:** Writing – original draft, Software, Data curation.

Author's Contributions

All authors contributed equally. All authors have read and agreed to this version of the manuscript.

Declaration of competing interest

The authors declare that they have no known competing financial interests or personal relationships that could have appeared to influence the work reported in this paper.

Acknowledgements

This work was supported by the National Natural Science Foundation of China (62376252); Key Project of Natural Science Foundation of Zhejiang Province (LZ22F030003); Zhejiang Province Leading Geese Plan (2025C02025, 2025C01056); Zhejiang Province Province-Land Synergy Program (2025SDXT004-3). The authors extend their appreciation to the Deanship of Research and Graduate Studies at King Khalid University for funding this work through Large Research Project under grant number RGP2/299/45". The authors extend their appreciation to the Deanship of Scientific Research at Northern Border University, Arar, KSA for funding this research work through the project number NBU-FPEJ-2025-2714-01. This work was supported by Princess Nourah bint Abdulrahman University Researchers Supporting Project number (PNURSP2025R236), Princess Nourah bint Abdulrahman University, Riyadh, Saudi Arabia.

Nomenclature

a	Constant
B (T)	Uniform magnetic field
B_0	Magnetic induction
\hat{C}	Flow concentration
C_p (J / (kg.K))	Specific heat at constant pressure
D_T	Thermophoretic diffusion parameter
D_B	Brownian Diffusion parameter
E_c	Eckert number
f	Dimensionless velocity
Gr	Grashof number
j (m^2/kg)	Micro- Inertia density
γ^*	Spin gradient viscosity
k (W / (m.K))	Thermal conductivity
K	Material Parameter
M	Magnetic parameter
ρC_p	Heat capacitance
Pr	Prandtl number
R^2	Regression value
Re	Local Reynolds number

s_0	Surface rotational Parameter
\hat{T}	Fluid temperature
$\hat{u} & \hat{v}$	Velocity components along \hat{x} & \hat{y} directions
$\hat{x} & \hat{y}$	Cartesian coordinate system
$\beta_t (K^{-1})$	Thermal Expansion coefficient
$\beta_c (K^{-1})$	Concentration expansion coefficient
η	Similarity variable
θ	Dimensionless temperature
ϕ	Dimensionless concentration
$\mu(Pa.s)$	Viscosity
$\rho (Kg/m^3)$	Density
$\vartheta (m^2/s)$	Kinematic viscosity
$\sigma (S/m)$	Electrical conductivity

Data availability

No data was used for the research described in the article.

References

- [1] L.J. Crane, Flow past a stretching plate, *J. Appl. Math. Phys.* 21 (1970) 645–647.
- [2] H.I. Andersson, Slip flow past a stretching surface, *Acta Mech.* 158 (1) (2002) 121–125.
- [3] J.G. Leishman, *Introduction to Aerospace Flight Vehicles*, 2023.
- [4] Shreedevi Madiwal, N.B. Naduvinamani, J.K. Madhukesh, Umair Khan, Anuar Ishak, Raman Kumar, Md Irfanul Haque Siddiqui, Computational role of autocatalytic chemical reaction in the dynamics of a ternary hybrid nanofluid past a rotating stretching surface, *Adv Math Phys.* 2024 (1) (2024) 1223917.
- [5] Shuguang Li, Rania Saadeh, J.K. Madhukesh, Umair Khan, G.K. Ramesh, Aurang Zaib, B.C. Prasannakumara, Raman Kumar, Anuar Ishak, M. Sherif El-Sayed, Aspects of an induced magnetic field utilization for heat and mass transfer ferromagnetic hybrid nanofluid flow driven by pollutant concentration, *Case Stud. Therm. Eng.* 53 (2024) 103892.
- [6] Umair Khan, Aurang Zaib, Javali K. Madhukesh, Samia Elattar, Sayed M. Eldin, Anuar Ishak, Zehba Raizah, Iskandar Waini, Features of radiative mixed convective heat transfer on the slip flow of nanofluid past a stretching bended sheet with activation energy and binary reaction, *Energies* 15 (20) (2022) 7613.
- [7] K. Karthik, Pudhari Srilatha, J.K. Madhukesh, Umair Khan, B.C. Prasannakumara, Raman Kumar, Anuar Ishak, Modassir Hussain Syed, Taseer Muhammad, M. Modather M. Abdou, Computational examination of heat and mass transfer of nanofluid flow across an inclined cylinder with endothermic/exothermic chemical reaction, *Case Stud. Therm. Eng.* 57 (2024) 104336.
- [8] J. Madhu, J.K. Madhukesh, I. Sarris, B.C. Prasannakumara, G.K. Ramesh, Nehad Ali Shah, Bagh Ali, et al., Influence of quadratic thermal radiation and activation energy impacts over oblique stagnation point hybrid nanofluid flow across a cylinder, *Case Stud. Therm. Eng.* (2024) 104624.
- [9] A.C. Eringen, Theory of micropolar fluids, *J. Math. Mech.* 16 (1966) 1–18.
- [10] M. Zadravec, M. Hriberek, L. Skerget, Natural convection of micropolar fluid in an enclosure with boundary element method, *Eng. Anal. Bound. Elem.* 33 (2009) 485–492.
- [11] G. Lukaszewicz, *Micropolar Fluids: Theory and Application*, Birkhauser, Boston, MA, USA, 1999.
- [12] A.C. Eringen, *Micro Continuum Field Theories: II* Fluent Media, Springer, Berlin/Heidelberg, Germany, 2001.
- [13] M. Israr Ur Rehman, Haibo Chen, Aamir Hamid, Haitao Qi, Numerical analysis of unsteady non-linear mixed convection flow of reiner-philippoff nanofluid along Falkner-Skan wedge with new mass flux condition, *Chem. Phys. Lett.* 830 (2023) 140799.
- [14] M. Israr Ur Rehman, Haibo Chen, Aamir Hamid, Shami AM. Alsallami, A. Al-Zubaidi, S. Saleem, Thermal and solutal slip impacts of tribological coatings on the flow and heat transfer of reiner-philippoff nanofluid lubrication toward a stretching surface: the applications of Darcy-Forchheimer theory, *Tribol. Int.* 190 (ID) (2023) 109038.
- [15] Ur Rehman, M. Israr, Haibo Chen, Aamir Hamid, Multi-physics modeling of magnetohydrodynamic Carreau fluid flow with thermal radiation and Darcy-Forchheimer effects: a study on Soret and Dufour phenomena, *J. Therm. Anal. Calorim.* 148 (24) (2023) 13883–13894.
- [16] Ur Rehman, M. Israr, Haibo Chen, Faisal Z. Duraihem, Mohamed Hussen, Aamir Hamid, Haitao Qi, Darcy-Forchheimer aspect on unsteady bioconvection flow of Reiner-Philippoff nanofluid along a wedge with swimming microorganisms and Arrhenius activation energy, *Numer. Heat Tran., Part A: Applications* (2024) 1–19.
- [17] M. Israr Ur Rehman, Haibo Chen, Aamir Hamid, Impact of bioconvection on Darcy-Forchheimer flow of MHD Carreau fluid with Arrhenius activation energy, *ZAMM-J Appl Math Mech /Zeitschrift für Angewandte Mathematik und Mechanik.* 104 (1) (2024) e202300164.
- [18] M. Israr Ur Rehman, Haibo Chen, Aamir Hamid, Kamel Guedri, Analysis of Cattaneo–Christov heat flux and thermal radiation on Darcy–Forchheimer flow of Reiner–Philippoff fluid, *Int. J. Mod. Phys. B* 38 (3) (2024) 2450046.
- [19] Haibo Chen, M. Israr Ur Rehman, Nek Muhammad Katbar, Aamir Hamid, Faisal Z. Duraihem, Qi Haitao, Effect of an inclined magnetic field on unsteady mixed convective stagnation point flow over a permeable stretching sheet with radiative heat transfer, *Phys. Scripta* 98 (9) (2023) 095255.
- [20] M. Israr Ur Rehman, Haibo Chen, Aamir Hamid, Kamel Guedri, Thabet Abdeljawad, Dezh Yang, Theoretical investigation of Darcy-Forchheimer flow of bioconvection Casson fluid in the presence of chemical reaction effect, *Biomass Conversion Biorefinery.* (2022) 1–11.
- [21] M. Israr Ur Rehman, Haibo Chen, Aamir Hamid, Wasim Jamshed, Mohamed R. Eid, Faisal Z. Duraihem, Haifa Alqahtani, Thermal analysis of radiative and electromagnetic flowing of hybridity nanofluid via Darcy-Forchheimer porous material with slippage constraints, *Energy Environ.* (2023) 0958305X231196298.
- [22] Ur Rehman, M. Israr, Haibo Chen, Aamir Hamid, Wasim Jamshed, Mohamed R. Eid, Hamiden Abd El-Wahed Khalifa, Almaz Ali Yousif Badria, Chemical reactive process of unsteady bioconvective magneto Williamson nanofluid flow across wedge with nonlinearly thermal radiation: Darcy-Forchheimer model, *Numer. Heat Tran., Part B: Fundamentals* 84 (4) (2023) 432–448.
- [23] M. Israr Ur Rehman, Haibo Chen, Aamir Hamid, Wasim Jamshed, Mohamed R. Eid, Sayed M. El Din, Hamiden Abd El-Wahed Khalifa, Assmaa Abd-Elmonem, Effect of Cattaneo-Christov heat flux case on Darcy-Forchheimer flowing of Sutterby nanofluid with chemical reactive and thermal radiative impacts, *Case Stud. Therm. Eng.* 42 (2023) 102737.
- [24] P. Pooya, M. Saeid, Z. Meysam, Application of numerical methods in micropolar fluid flow and heat transfer in permeable plates, *Alex. Eng. J.* 61 (4) (2022) 2663–2672.

- [25] J. Chen, C. Liang, J.D. Lee, Theory and simulation of micropolar fluid dynamics, *Proc. Inst. Mech. Eng. - Part N J. Nanoeng. Nanosyst.* 224 (1–2) (2010) 31–39.
- [26] A. Alsaedi, H. Tasawar, Q. Sumaira, Y. Rabiya, Eyring-Powell nanofluid flow with nonlinear mixed convection: entropy generation minimization, *Comput. Methods Progr. Biomed.* 186 (2020) 105183.
- [27] T. Hayat, Q. Sumaira, A. Ahmed, A. Bashir, Entropy generation minimization: Darcy-Forchheimer nanofluid flow due to curved stretching sheet with partial slip, *Int. Commun. Heat Mass Tran.* 111 (2020) 104445.
- [28] P. Li, L. Chen, S. Xia, et al., Total entropy generation rate minimization configuration of a membrane reactor of methanol synthesis via carbon dioxide hydrogenation, *Sci. China Technol. Sci.* 65 (2022) 657–678.
- [29] P. Mondal, T.R. Mahapatra, MHD double-diffusive mixed convection and entropy generation of nanofluid in a trapezoidal cavity, *Int. J. Mech. Sci.* 208 (2021) 106665.
- [30] E.O. Fatunmbi, A. Adeniyi, Nonlinear thermal radiation and entropy generation on steady flow of magneto-micropolar fluid passing a stretchable sheet with variable properties, *Res Eng.* 6 (2020) 100142.
- [31] K. Singhv, A.K. Pandey, M. Kumar, Entropy generation impact on flow of micropolar fluid via an inclined channel with non-uniform heat source and variable fluid properties, *Int J Appl Comput Math.* 6 (85) (2020).
- [32] E.O. Fatunmbi, S.O. Salawu, Thermodynamic second law analysis of magneto-micropolar fluid flow past nonlinear porous media with non-uniform heat source, *Propulsion Power Res.* 9 (3) (2020) 281–288.
- [33] P.K. Yadav, A. Kumar, An inclined magnetic field effect on entropy production of non-miscible Newtonian and micropolar fluid in a rectangular conduit, *Int. Commun. Heat Mass Tran.* 124 (2021) 105266.
- [34] D. Srinivasacharya, K.H. Bindu, Entropy generation in a micropolar fluid flow through an inclined channel with slip and convective boundary conditions, *Energy* 91 (2015) 72–83.
- [35] S.K. Asha, C.K. Deepa, Entropy generation for peristaltic blood flow of a magneto-micropolar fluid with thermal radiation in a tapered asymmetric channel, *Res Eng.* 3 (2019) 100024.
- [36] J. Srinivas, Ramana M. Jv, J.C. Ali, Analysis of entropy generation in an inclined channel flow containing two immiscible micropolar fluids using HAM, *Int. J. Numer. Methods Heat Fluid Flow* 26 (3/4) (2016) 1027–1049.
- [37] B. Yegnanarayana, Artificial Neural Networks, PHI Learning Pvt. Ltd., 2009.
- [38] J. Zou, Yi Han, Sung-San So, Overview of artificial neural networks. *Artificial Neural Networks: Methods and Applications*, 2009, pp. 4–22.
- [39] B. Wang, W. Jingtao, Application of artificial intelligence in computational fluid dynamics, *Ind. Eng. Chem. Res.* 60 (7) (2021) 2772–2790.
- [40] I. Khan, U. Hakeem, A. Hussain, F. Mehreen, I. Saeed, S. Muhammad, A. Muhammad, G. Abdu, I. Farkhanda, Fractional analysis of MHD boundary layer flow over a stretching sheet in porous medium: a new stochastic method, *J Function Spaces.* 2021 (2021) 1–19.
- [41] A. García-Gutiérrez, D. Domínguez, D. López, J. Gonzalo, Atmospheric boundary layer wind profile estimation using neural networks applied to lidar measurements, *Sensors* 21 (11) (2021) 3659.
- [42] M.A.Z. Raja, S. Azad, S.M. Shah, Bio-inspired computational heuristics to study the boundary layer flow of the Falkner-Scan system with mass transfer and wall stretching, *Appl. Soft Comput.* 57 (2017) 293–314.
- [43] M. Israr Ur Rehman, Haibo Chen, M. Imran Khan, Aamir Hamid, Atef Masmoudi, Modeling and predicting heat transfer performance in bioconvection flow around a circular cylinder using an artificial neural network approach, *Tribol. Int.* 200 (ID) (2024) 110182.
- [44] Syed Zahir Hussain Shah, Shabeer Khan, Rania Saadeh, Hafiz Abdul Wahab, Javali Kotresh Madhukesh, Umair Khan, Anuar Ishak, Syed Modassir Hussain, On the thermal performance of a three-dimensional cross-ternary hybrid nanofluid over a wedge using a Bayesian regularization neural network approach, *High Temp. Mater. Process.* 43 (1) (2024) 20240051.
- [45] Surbhi Sharma, Amit Dadheeck, Amit Parmar, Jyoti Arora, Qasem Al-Mdallal, S. Saranya, MHD micro polar fluid flow over a stretching surface with melting and slip effect, *Sci. Rep.* 13 (1) (2023) 10715.
- [46] Muhammad Waqas, Muhammad Farooq, Muhammad Ijaz Khan, Alsaedi Ahmed, Tasawar Hayat, Tabassum Yasmeen, Magnetohydrodynamic (MHD) mixed convection flow of micropolar liquid due to nonlinear stretched sheet with convective condition, *Int. J. Heat Mass Tran.* 102 (2016) 766–772.
- [47] M. Sheikholeslami, R. Ellahi, H.R. Ashorynejad, G. Domairry, T. Hayat, Effects of heat transfer in flow of nanofluids over a permeable stretching wall in a porous medium, *J. Comput. Theor. Nanosci.* 11 (2) (2014) 486–496.
- [48] M. Bilal, A. Saeed, T. Gul, Parametric simulation of micropolar fluid with thermal radiation across a porous stretching surface, *Sci. Rep.* 12 (2022) 2542, et al.
- [49] K. Rafique, M.I. Anwar, M. Misiran, I. Khan, D. Baleanu, K.S. Nisar, E.S.M. Sherif, A.H. Seikh, Hydromagnetic flow of micropolar nanofluid, *Symmetry* 12 (2) (2020) 251.
- [50] Rafael Cortell, Viscous flow and heat transfer over a nonlinearily stretching sheet, *Appl. Math. Comput.* 184 (2) (2007) 864–873.
- [51] K. Vajravelu, Viscous flow over a nonlinearily stretching sheet, *Appl. Math. Comput.* 124 (3) (2001) 281–288.
- [52] A. Roja, B.J. Gireesha, B.C. Prasannakumara, MHD micropolar nanofluid flow through an inclined channel with entropy generation subjected to radiative heat flux, viscous dissipation and multiple slip effects, *Multidiscip. Model. Mater. Struct.* 16 (6) (2020) 1475–1496.